STATISTICAL ANALYSIS OF MECHANICAL DAMAGE IN NANOPILLAR ARRAYS WITH MIXED-MODE LOAD TRANSFER

Tomasz Derda

Institute of Mathematics, Czestochowa University of Technology
Czestochowa, Poland
tomasz.derda@im.pcz.pl

Abstract. In the framework of the Fibre Bundle Model we explore the effect of mixed--mode load transfer in two-dimensional arrays of nanopillars. The mixed-mode load redistribution scheme serves as an interpolation between limiting cases, namely global and local transfer. Two types of loading processes are employed i.e. quasi-static and sudden loading. By varying the weight parameter, we identify two behaviours: the GLS and LLS regime. As a regime indicator we use distribution of critical loads and function fitting probability of system breakdown.

1. Introduction

The phenomena of failure and fracture of materials are a complex collection of phenomena in science and engineering. For the reason of the disorder in the materials and their inherent nonuniformity, the failure processes of real materials usually cannot be described by simple linear equations. Therefore, statistical models are widely used to study the fracture and breakdown processes. One of the most important theoretical approaches is the fibre bundle model (FBM) [1-3], which illustrates a stochastic fracture-failure process in disordered materials subjected to external load. The key aspect of the FBM is a load transfer rule which is responsible for the mechanism of redistribution of load carried by the broken fibres (elements) to the intact ones. The load sharing rules can be divided into two extreme classes: global load sharing (GLS) and local load sharing (LLS). In the GLS model, long-range interactions are assumed as all the intact elements equally share a load of a failed element. The LLS model represents short-range interactions

- the load from the destroyed element is redistributed only to its nearest intact neighbours. Both of these rules are idealised cases, hence Pradhan et al. [4] proposed the mixed-mode load sharing rule and explored it for one-dimensional case.

In this work, using the mixed-mode FBM, we analyse chosen quantities of damage processes in arrays of vertical nanopillars distributed on a flat substrate. The paper is organised as follows. The model is described in the next section. Then, simulation results are presented and discussed. In the final section our findings are summarised briefly.

2. Model

We consider the system as a set of N longitudinal nanopillars located in the nodes of the supporting lattice. We analyse only regular arrangements i.e. hexagonal, square and triangular grids. However, the main interest is devoted to the square lattice case, which is seen as a set of $N = L \times L$ pillars with L being the linear dimension. If it not specified otherwise, we explore the square lattice case.

Each pillar is characterised by its own strength threshold to an applied axial load. The existence of defects in actual materials plays a key role in the mechanical response of materials under load. Hence, pillar-strength-thresholds σ_{th}^{i}, $i = 1,2,..,N$ are quenched random variables distributed according to the two-parameter Weibull distribution

$$P(\sigma_{th}) = 1 - \exp\left\{-\left(\frac{\sigma_{th}}{\lambda}\right)^{\rho}\right\} \qquad (1)$$

where ρ is the shape parameter, also known as the Weibull index, and λ is the scale parameter. The first parameter controls the amount of disorder in the system. In this work we assume $\lambda = 1$ and $\rho = 2$, which means strong disorder.

The system is subjected to axial external loading. In the following simulation it is instructive to consider two different, but also equivalent, loading procedures: quasi-static loading and sudden loading (finite force application). For both of these processes the uniform loading is assumed, however, the internal load transfers can cause inhomogeneities in loads of individual pillars.

In the case of quasi-static loading the external load F is gradually increased up to the complete failure of the system. Initially the system is unloaded and intact. Then the load is uniformly increased on all the working pillars just to destroy the weakest one. Then, the increase of the external load is stopped and the load from the destroyed pillar is transferred to intact pillars. The load redistribution may lead to subsequent pillar failures which can provoke the next failures. A stable state is achieved if the load redistribution does not cause any failures. In such a situation, the external load has to be increased again. The above described dynamics is continued until destruction of all pillars.

Sudden loading of the system is realised by application of an external force F which is kept constant during the entire loading process. Due to uniform loading, in the moment of application of load F the load per pillar is $\sigma = F / N$, so all the pillars with strength thresholds smaller than σ are immediately destroyed. Then, the load transfers may lead to the next failures. This procedure leads to a stable state of the system which is either partially or fully destroyed. The third possibility is that the system is intact - only if σ is not greater than σ_{th} of the weakest pillar.

As a load transfer rule, we apply mixed-mode load sharing with weight parameter g. In this scheme, when a pillar fails, fraction g of its load is transferred locally and the rest ($1 - g$ fraction) is distributed globally. Therefore, the mixed-mode load sharing is an interpolation mechanism between the GLS and LLS − $g = 0$ corresponds to the GLS rule and $g = 1$ represents the pure LLS rule.

3. Analysis of the simulation results

Based on the model presented in the previous section, we have developed program codes for simulation of damage processes in the nanopillar arrays. Then, we have performed intensive computer simulations. Generally, we study the behaviour of the model from $g = 0$ up to $g = 1$ with a step of 0.05. Because of computational time limitations, in some cases we increase step to 0.1.

3.1. Quasi-static loading

For the quasi-static loading, the damage process proceeds in an avalanche-like manner. Although initial load increases provoke only single pillar failures, further load increases involve bursts of failures. Such a single failure or a burst of pillar failures caused by load increase is called an avalanche (Δ). Application of quasi-static loading process ensures obtaining the minimum external load F that is needed to induce catastrophic avalanche Δ_c which contains all previously undestroyed pillars. Therefore, we can find the maximum value of applied load F_c (total critical load) that can be supported by the system. The strength of the bundle can be scaled by the system size, thus giving critical load per pillar $\sigma_c = F_c / N$.

For the GLS rule, we assume that the support-pillar interface is perfectly rigid, whereas, in the case of the LLS rule, this support has a certain compliance. Thus, for the GLS all the intact pillars are under equal load and the geometry of lattice is irrelevant. This is in contrast to the LLS rule, where load redistribution is localized and distribution of load is not homogeneous. By increasing g, load transfer changes from pure long-range ($g = 0$) to strictly localized ($g = 1$). In the following we analyse how it influences the mean value of critical load σ_c.

It is known from [5-7] that for the Weibull distributed elements and the GLS rule the mean critical load $\langle \sigma_c \rangle$ asymptotically tends to:

$$\langle \sigma_c \rangle \xrightarrow[N \to \infty]{} \rho^{-1/\rho} e^{-1/\rho} . \tag{2}$$

Different behaviour is observed for the LLS scheme - $\langle \sigma_c \rangle$ tends to zero in the asymptotic limit. We have found that $\langle \sigma_c \rangle$ can be nicely fitted by the function [8]:

$$\langle \sigma_c \rangle = \frac{\beta}{(\ln N)^\delta} . \tag{3}$$

with $\beta = 0.671$ and $\delta = 0.35$. These values of the parameters were not published yet. Formula (3) concerns two-dimensional square grids and was originally fitted to systems with uniformly distributed pillar-strength-thresholds.
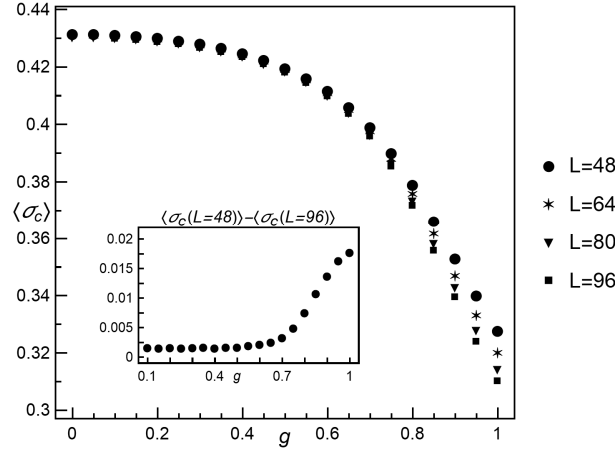

Fig. 1. The mean critical load versus weight parameter g for different system sizes. The averages are taken from at least 5000 samples for each presented value. In the inset we show the results of subtracting $\langle \sigma_c \rangle$ for $L = 48$ from $\langle \sigma_c \rangle$ for $L = 96$

In Figure 1 we have plotted, for different system sizes, the mean critical load $\langle \sigma_c \rangle$ as a function of weight parameter g. The function is strictly decreasing - as g is increased, the load transfer becomes more and more localised which causes weakening of the system. It is also seen that for $g \leq 0.65$ values of $\langle \sigma_c \rangle$ are almost identical irrespective of the system size, and this suggests dominance of long-range interactions (GLS regime). Then, for higher values of g the differences between $\langle \sigma_c \rangle$ for presented system sizes noticeably increase (see inset in Figure 1). From

$g = 0.8$ we distinctly observe a size-dependent behaviour which is an evidence of LLS regime dominance. The similar behaviour was reported by Pradhan et al. [4], but the results are not directly comparable, because their results concern a one-dimensional model with uniformly distributed strength-thresholds.

To analyse the influence of pillar arrangements, we compare the results of $\langle \sigma_c \rangle$ for three regular lattices (see Figure 2). Each lattice is characterised by its own number of nearest neighbours, namely hexagonal - 3, square - 4 and triangular - 6. In the classical LLS scheme, as the number of nearest neighbours increases the load from the destroyed pillar becomes more dispersed and thus leads to a strengthening of the system. For the LLS the hexagonal system is the weakest, while the triangular system is the strongest one. The same behaviour is observed for the mixed-mode $(g > 0)$ although, for smaller values of g, the differences are close to 0. From $g = 0.5$, the results for hexagonal lattice start to visibly differ from the results obtained for square and triangular geometries, while the results for these two geometries are almost equal up to $g = 0.8$.
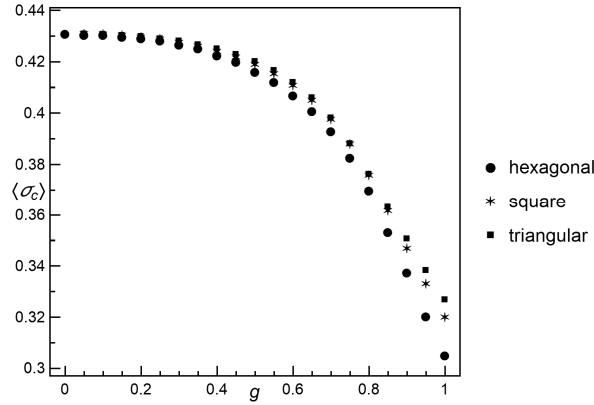

Fig. 2. The mean critical load as a function of weight parameter g for different system geometries and $N = 64^2$. The averages are taken from at least 5000 samples for each presented value

In our previous works, we have noticed that for the LLS model the distribution of σ_c can be fitted by three-parameter skew normal distribution (SND) with probability density function [9, 10]:

$$p(\sigma_c) = \frac{\exp\left[-\dfrac{(\sigma_c - \xi)^2}{2\omega^2}\right] \mathrm{erfc}\left[-\dfrac{\alpha(\sigma_c - \xi)}{\sqrt{2}\omega}\right]}{\sqrt{2\pi}\omega} \tag{4}$$

and cumulative distribution function (CDF)

$$P\left(\sigma_c\right) = \frac{1}{2}\mathrm{erfc}\left(-\frac{\sigma_c - \xi}{\sqrt{2}\omega}\right) - 2\mathrm{T}\left(\frac{\sigma_c - \xi}{\omega}, \alpha\right) \tag{5}$$

where ξ, ω, α are location, scale and shape parameters, respectively. Function $\mathrm{erfc}(z)$ represents a complimentary error function and $\mathrm{T}(x,a)$ is Owen's T function.

In the case of the GLS model, distribution of σ_c follows normal distribution. Skew normal distribution is a generalisation of normal distribution for non-zero skewness. Therefore, we have fitted distribution of σ_c for the mixed-mode scheme by skew normal distribution. But first, in Figure 3, we present results of skewness of σ_c distribution for different values of g and chosen system sizes. We can see that up to $g = 0.7$ distribution of σ_c is approximately symmetric. From $g = 0.7$ up to $g = 1$ skewness is negative like in the LLS case and moderate skewness is approached.
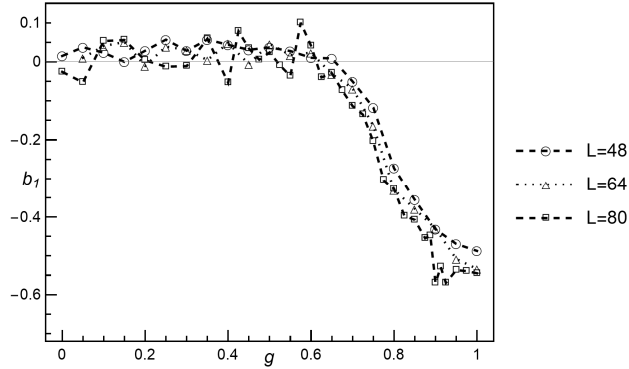

Fig. 3. The skewness of critical load as a function of weight parameter g for different system sizes. The results are taken from at least 5000 samples for each presented value
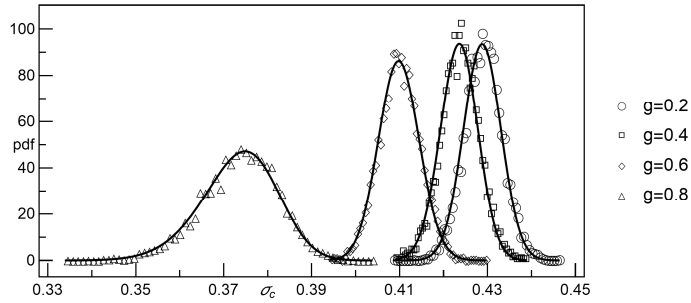

Fig. 4. Empirical probability density functions of the σ_c in an array of 80×80 pillars. The solid lines represent probability density function of skew normally distributed σ_c with parameters computed from the samples
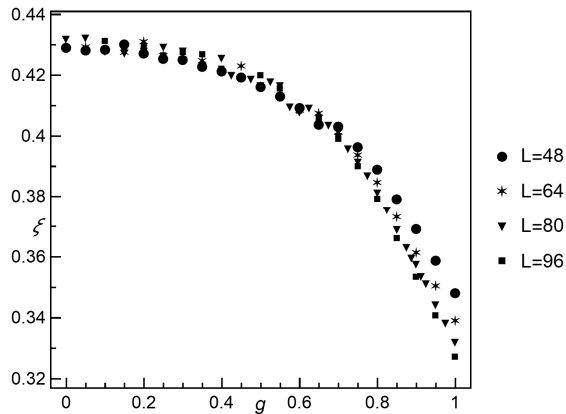
Fig. 5. The location parameter ξ of skew normal distribution as a function of g for different system sizes
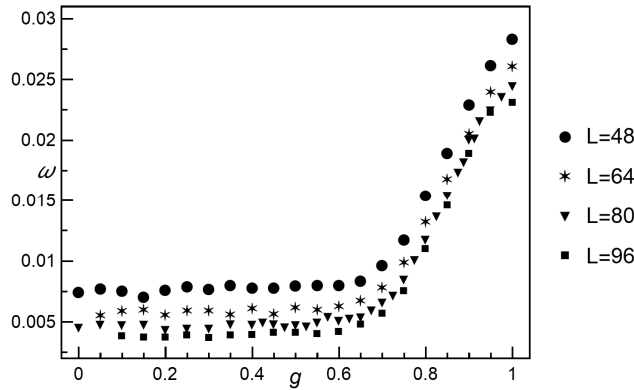

Fig. 6. The scale parameter ω of skew normal distribution as a function of g for different system sizes

Figure 4 illustrates exemplary empirical probability density functions of σ_c for different values of weight parameter g. Figures 5-7 graphically report fitted values of parameters of skew normally distributed σ_c. Each presented result is based on at least 20,000 independent samples ($L = 48$), 10,000 samples ($L = 64$) and 5,000 samples ($L = 80$ and $L = 96$). In Figure 4, two regimes can be noticed. For $g \leq 0.6$ we see three curves similar to each other in terms of dispersion, which is low in comparison to dispersion for $g = 0.8$. This observation is supported by Figure 6, where a noticeable increase of estimated scale parameter ω is observed from $g = 0.7$ up to $g = 1$, whereas up to $g = 0.6$ fitted values of ω are almost constant. Figure 7 depicts estimated values of shape parameter α. Up to $g = 0.65$ values of α are scattered around zero in the range of approximately $(-1,1)$. From $g = 0.7$ up

to $g = 1$, values of α generally decrease and all are negative. It thus allows us to clearly differentiate between two regimes. We have also tested a hypothesis about normal distribution of σ_c (significance level of 0.05). The hypothesis was not rejected up to $g = 0.7$ for all analysed system sizes. From $g = 0.75$ up to $g = 1$ all cases were rejected.
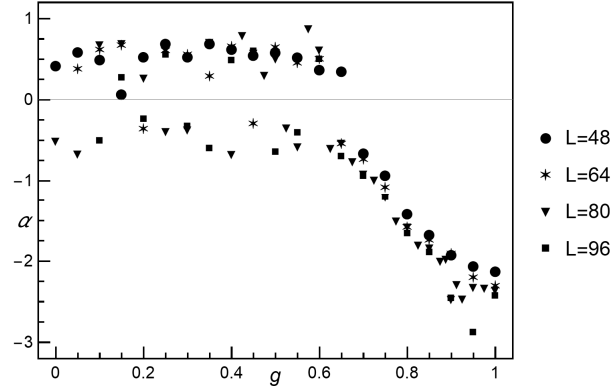

Fig. 7. The shape parameter α of skew normal distribution as a function of g for different system sizes

3.2. Sudden loading

In this subsection we analyse probabilities of breakdown (P_b) of systems loaded by finite force F. Application of $\sigma = F / N$ allows us to compare results for different system sizes. Figure 8 depicts empirical breakdown probabilities for chosen values of weight parameter g. It is seen that fitted curves are ordered according to g. In addition, the distance (in the x-direction) between consecutive curves seems to increase as g is increased. For $g \leq 0.7$ the fitted curves sharply increase, whereas for $g = 0.8$ and $g = 0.9$, values of P_b increase more slowly.

For fitting our data we employ cumulative distribution function of skew normal distribution, and thus we rewrite formula (5):

$$P_b(\sigma) = \frac{1}{2}\text{erfc}\left(-\frac{\sigma - \xi_{SL}}{\sqrt{2}\omega_{SL}}\right) - 2\text{T}\left(\frac{\sigma - \xi_{SL}}{\omega_{SL}}, \alpha_{SL}\right) \qquad (6)$$

Figures 9-11 show fitted values of parameters ξ_{SL}, ω_{SL} and α_{SL} for different system sizes. It can be noticed that the behaviour of these parameters is very similar to the behaviour of their counterparts in the case of quasi-static loading. This proves that the two applied loading procedures are equivalent.
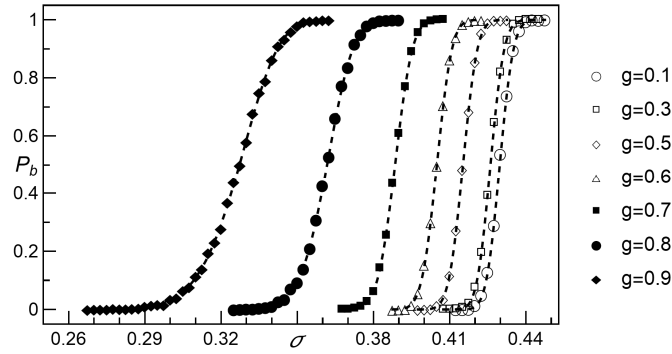
Fig. 8. Empirical breakdown probability P_b as a function of initial load per pillar σ for different values of weight parameter g. All presented data are calculated from 2000 statistically independent samples. System size $N = 80 \times 80$. The dashed lines represent function (6) with parameters computed from simulations
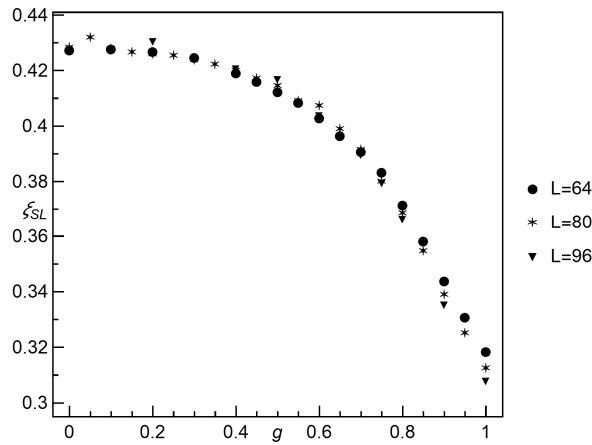

Fig. 9. The parameter ξ_{SL} of formula (6) as a function of g for different system sizes

   The dominance of short range interactions is distinctly visible for $g > 0.7$ (see Figures 10 and 11). The GLS regime dominates up to $g = 0.65$.
   At the beginning of the section, we have mentioned about distances between curves for consecutive values of g. Quartile can serve as a tool to measure the distance in the x-direction. Using values of parameters ξ_{SL}, ω_{SL} and α_{SL} we compute quartiles of the skew normal distribution. Then we calculate differences between quartiles for $g - 0.05$ and for g. By that means we obtain distances between consecutive curves with step of 0.05. The results are plotted in Figure 12. It is seen that the distance between consecutive curves is an increasing function up to $g = 0.9$, then distance start to decrease. This behaviour shows that for $g = 0.9$ short

range interactions in the system are so prevalent that further increase of g is less significant.
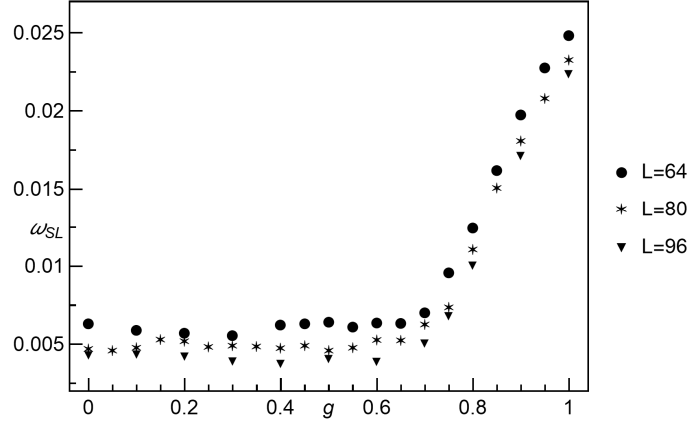

Fig. 10. The parameter ω_{SL} of formula (6) as a function of g for different system sizes
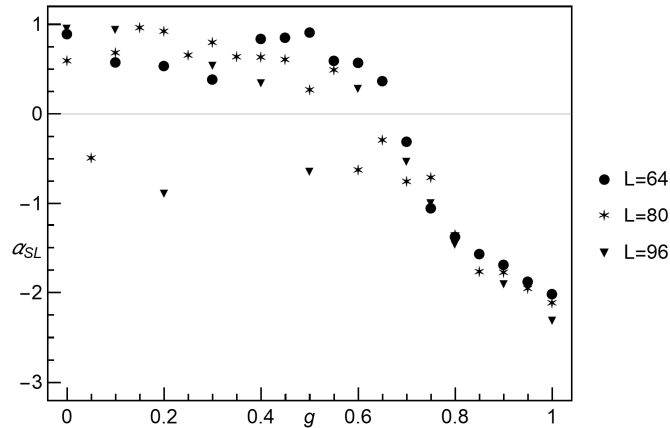

Fig. 11. The parameter α_{SL} of formula (6) as a function of g for different system sizes

Finally, we compare approximations of P_b by cumulative distribution functions of two distributions, namely normal and skew normal. To study the quality of approximation we apply the mean absolute error (MAE). The results of MAE are reported in Figure 13. Up to $g = 0.65$ both of the functions generate almost equal errors (GLS regime), then mean absolute errors for normal distribution are greater than their skew-normal counterparts (LLS behaviour). From $g = 0.8$ the difference is becoming considerable and thus suggesting distinct LLS regime.
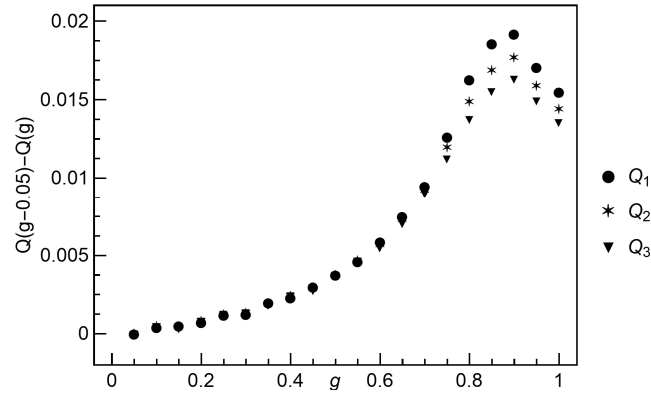
Fig. 12. The results of subtracting quartile of SND for $g - 0.05$ from quartile of SND for g. Parameters of SND are based on the simulation results. The results concern systems with $N = 80 \times 80$ pillars
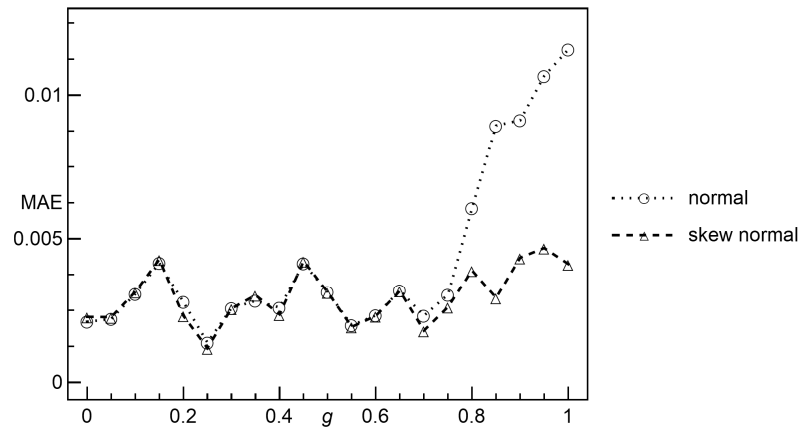

Fig. 13. Mean absolute errors of P_b approximation using: CDF of the SND and CDF of the normal distribution. The results concern systems with $N = 80 \times 80$ pillars

4. Conclusions

By means of numerical simulation, we have studied breakdown processes in the mixed-mode load transfer model of nanopillar arrays subjected to external load. This model is completely GLS scheme for weight parameter $g = 0$ and pure LLS scheme for $g = 1$.

Application of two different loading procedures allowed us to analyse two quantities i.e. critical load and breakdown probability. We have shown that distribution of critical load can be nicely fitted by the skew normal distribution, and breakdown probability is well approximated by the cumulative distribution func-

tion of this distribution. The parameters of the these functions can serve as the indicators of the system regime. We have tuned values of g from 0 to 1 with step of 0.05. We have observed that up to $g = 0.65$ long range interactions prevail (GLS behaviour), whereas from $g = 0.8$ we see distinct LLS behaviour with short range interactions. Between the two mentioned above values of g, the crossover regime is present.

In the future work we are planning to investigate critical loads and breakdown probabilities in the heterogeneous load sharing model proposed by Biswas and Chakrabarti [12]. In this model, the system is divided into two groups of elements in which part of the elements is characterised by completely local behaviour and the rest follows the global load sharing scheme which means that it is also an interpolation scheme between LLS and GLS.

References

[1] Hansen A., Hemmer P.C., Pradhan S., The Fiber Bundle Model: Modeling Failure in Materials, Wiley, 2015.

[2] Alava M.J., Nukala P.K.V.V., Zapperi S., Statistical models of fracture, Adv. in Physics 2006, 55, 349-476.

[3] Pradhan S., Hansen A., Chakrabarti B.K., Failure processes in elastic fiber bundles, Rev. Mod. Phys. 2010, 82, 499-555.

[4] Pradhan S., Chakrabarti B.K., Hansen A., Crossover behavior in a mixed-mode fiber bundle model, Phys. Rev. E 2005, 71, 036149.

[5] McCartney L.N., Smith R.L., Statistical theory of the strength of fiber bundles, J. Appl. Mech. 1983, 50(3), 601-608.

[6] Smith R.L., The asymptotic distribution of the strength of a series-parallel system with equal load-sharing, The Annals of Probability 1982, 10(1), 137-171.

[7] Porwal P.K., Beyerlein I.J., Phoenix S.L., Statistical strength of a twisted fiber bundle: an extension of Daniels equal-load-sharing parallel bundle theory, Journal of Mechanics of Materials and Structures 2006, 1(8), 1425-1447.

[8] Domański Z., Derda T., Sczygiol N., Critical Avalanches in Fiber Bundle Models of Arrays of Nanopillars, Proceedings of the International MultiConference of Engineers and Computer Scientists 2013, Vol. II, IMECS 2013, March 13-15, 2013.

[9] Derda T., Stochastic local load redistribution in the fibre bundle model of nanopillar arrays, J. Appl. Math. Comput. Mech. 2015, 14(4), 19-30.

[10] Domański Z., Derda T., Distributions of Critical Load in Arrays of Nanopillars, Proceedings of the World Congress on Engineering (WCE 2017), Vol. II, 797-801.

[11] Derda T., Avalanche statistics in transfer load models of evolving damage, Scientific Research of the Institute of Mathematics and Computer Science 2011, 10(1), 21-31.

[12] Biswas S., Chakrabarti B.K., Crossover behaviors in one and two dimensional heterogeneous load sharing fiber bundle models, Eur. Phys. J. B 2013, 86, 160.